Thermal diffusion and mixture separation in the acoustic boundary layer

G. W. Swift and P. S. Spoor

Condensed Matter and Thermal Physics Group, Los Alamos National Laboratory, Los Alamos, New Mexico 87545

Oscillating thermal diffusion in a sound wave in a mixture of two gases is remarkably effective for separating the components of the mixture. We consider this separation process in boundary-layer approximation, with zero temperature gradient and zero concentration gradient along the direction of sound propagation. In the boundary layer, the combination of thermal diffusion with the oscillating temperature gradient and oscillating velocity gradient leads to second-order time-averaged fluxes of the two components of the mixture in opposite directions, parallel to the wave-propagation direction. The oscillating thermal diffusion also adds to the dissipation of acoustic power in the boundary layer, modifying thermal-relaxation dissipation but leaving viscous dissipation unchanged. © *1999 Acoustical Society of America.* [S0001-4966(99)03110-0]

PACS numbers: 43.35.Ud [HEB]

INTRODUCTION

In experiments on mode locking in acoustically coupled acoustic resonators,[1] we observed an anomalous difference in the resonance frequencies of the two resonators when using a He–Xe mixture. This frequency difference, up to 3% of the resonance frequency, was too large to be explained by any known difference between the resonators, such as temperature or geometry. We concluded that the sound wave in the acoustic coupler was separating the helium and xenon, thereby enriching one resonator with helium and the other with xenon.

We realized that this mass separation could be due to the mechanism illustrated in Fig. 1, which shows how the mixture can be separated by a combination of three effects in the boundary layers: oscillating temperature gradients in the thermal boundary layer, thermal diffusion, and oscillating velocity gradients in the viscous boundary layer. In a typical mixture of helium and xenon, the Prandtl number σ is about 1/4, so the viscous penetration depth δ_ν is about half the thermal penetration depth δ_κ, as shown in Fig. 1. For standing-wave phasing in a channel whose diameter is much larger than these penetration depths, we might think of the wave as consisting of the four steps equally spaced in time shown in Fig. 1(a)–(d). In the first step, while the pressure is high, the time-dependent part of the temperature has a steep gradient within δ_κ of the boundary as shown at the bottom of Fig. 1(a), due to the adiabatic temperature rise in the gas far from the wall and the large solid heat capacity of the wall itself. During this time, thermal diffusion drives the heavy component down the temperature gradient toward the boundary and the light component up the temperature gradient away from the boundary. (Signs may differ for different gases.) Hence, at the end of this time the gas near the solid boundary is enriched in the heavy component and depleted of the light component, while the gas approximately δ_κ from the solid boundary is enriched in the light component and depleted of the heavy component. In the second step, the gas moves upward, with a steep gradient of velocity within δ_ν of

the solid boundary due to viscosity, as shown at the bottom of Fig. 1(b). During this time, the heavy-enriched gas is relatively immobilized in the viscous boundary layer, while the light-enriched gas, just outside of the viscous boundary layer, moves easily upward. In the third step, shown in Fig. 1(c), low pressure reverses the sign of the temperature gradient, so the thermal diffusion reverses direction, forcing the heavy component away from the boundary and the light component toward the boundary. Thus in the fourth step, shown in Fig. 1(d), light-enriched gas is relatively immobilized while heavy-enriched gas moves easily downward. The net effect of these four steps is that some of the heavy component moves downward while some of the light component moves upward, as shown in Fig. 1(e).

Separation of gas mixtures using a sound wave has been observed earlier[2] and was attributed both to barodiffusion and thermal diffusion,[3] but with the latter involving the interaction of the second-order, time-averaged boundary-layer temperature gradient with the ordinary, second-order Rayleigh streaming.[4] We suspect that this fourth-order separation mechanism is generally weaker than our second-order process. Acoustic separation in mixtures of three gases using the differences between the ordinary mass diffusivities of two of the components through the third component has also been described[5] by Howell. This mechanism works independently of the boundary-layer temperature gradients and thermal diffusion of our process. Thermoacoustic condensation and evaporation of one component in a gas mixture have also been studied[6] by Raspet *et al.*, with oscillating mass diffusion of the condensing component.

Here, we present the first theoretical steps in support of the process illustrated in Fig. 1. To investigate a simple case, we restrict our analysis to the boundary-layer approximation in a two-component gas, and we assume that time-averaged temperature gradients and concentration gradients parallel to the direction of wave propagation are negligible.

After a brief introduction to the relevant length scales in the problem, we derive the oscillating temperature and oscil-
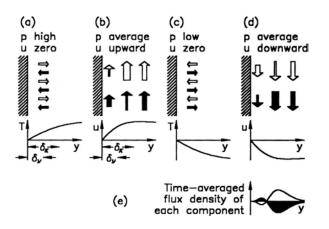
FIG. 1. Schematic of a possible separation process near a solid boundary in a standing wave, in a gas mixture with Prandtl number $\sigma \sim 1/4$. The solid arrows show motion of the heavy component, and the light arrows show motion of the light component. The lengths of the arrows represent velocity, and the widths of the arrows represent the local concentration of the components. As described in the text, (a) through (d) show processes occurring at time intervals separated by 1/4 of the period of the sound wave. The net result, shown in (e), is flux of the light component upward and flux of the heavy component downward.

lating concentration in a binary ideal gas mixture in boundary-layer approximation. We find that significant concentration oscillations exist, but with a different phasing than that suggested by Fig. 1. Next, we derive an expression for the second-order separation flux. The molar separation rate is surprisingly large for He–Xe and He–Ar mixtures, of order $10^{-3} M^2 a$, where M is the acoustic Mach number and a is the sound speed, suggesting that this process might be practical for deliberate separation of gas mixtures. The spectrum of practical applications requiring separation of mixtures is broad, including large-scale industrial processes such as petroleum refining, air separation, and beverage processing, and smaller-scale processes such as isotope separation and chemical analysis. A large number of ''physical'' mixture-separation techniques[7] are well understood and in widespread use, including time-independent thermal diffusion, ordinary diffusion, fractional distillation, centifugation, electromagnetic separation, chromatography, and superfluid heat flush. Much work remains in order to evaluate whether thermoacoustic mixture separation might find a useful niche in this vast industry. If so, we anticipate apparatus resembling thermoacoustic refrigerators,[8] with the large surface area of the stack (in which pore dimensions are a few times the thermal penetration depth) providing a large separation rate, and with feedstock entering and products leaving the acoustic system at standing-wave nodes.[9]

Next, we derive an expression for dissipation of acoustic power, showing that thermal diffusion adds slightly to the well-known viscous and thermal-relaxation dissipation mechanisms. Although the contribution of thermal diffusion to *bulk* attenuation of sound in gas mixtures is well known,[10] we have found only one published discussion[2] of this effect for boundary-layer attenuation.

It will be important to extend this work beyond the restrictive assumptions we have used here, in order to evaluate the phenomenon's usefulness for practical mixture separation and its effect on acoustic power dissipation/production

and enthalpy flux in the stacks of thermoacoustic engines and refrigerators[8] using gas mixtures.[11,12] These devices do not operate in the boundary-layer regime, and axial time-averaged temperature gradients always exist and concentration gradients may in fact exist. Until the present work is suitably extended, thermoacoustics calculations (using codes such as DeltaE[13] versions 1 through 4) for gas mixtures cannot be trusted.

I. IMPORTANT LENGTH SCALES

We will consider oscillations in a channel, in which all variables oscillate sinusoidally with time at frequency f. The wavelength $\lambda = a/f$, where a is the sound speed, is an important length scale, especially in the direction x of the gas displacement oscillations, and is much larger than all other length scales in the problem. The amplitude of the gas displacement oscillations in the x direction is a second important length scale, which typically is much smaller than both the wavelength and the length of the channel.

In the direction y perpendicular to the gas displacement oscillations, one key length scale is the thermal penetration depth

$$\delta_\kappa = \sqrt{2k/\omega \rho c_p} = \sqrt{2\kappa/\omega}, \tag{1}$$

where k is the thermal conductivity of the gas, ρ is its density, c_p is its isobaric heat capacity per unit mass, κ is its thermal diffusivity, and $\omega = 2\pi f$ is the angular frequency. The thermal penetration depth is approximately the distance that heat diffuses through the gas in a time $1/\pi f$. Gas much farther than this from the nearest solid surface experiences adiabatic oscillations, and will not participate in thermoacoustic effects. Closely related to the thermal penetration depth is the viscous penetration depth

$$\delta_\nu = \sqrt{2\mu/\omega \rho} = \sqrt{2\nu/\omega}, \tag{2}$$

where μ is viscosity and ν is kinematic viscosity. Within δ_ν of solid surfaces, viscous shear forces cause gradients in the oscillating velocity and displacement. In gas mixtures, a third key length scale is the mass-diffusion penetration depth

$$\delta_D = \sqrt{2D/\omega}, \tag{3}$$

where D is the binary mass diffusion coefficient (called D_{12} in some literature).

The Prandtl number

$$\sigma = \mu c_p/k = (\delta_\nu/\delta_\kappa)^2 \tag{4}$$

is a dimensionless measure of the ratio of viscous to thermal effects, which is near 2/3 for pure monatomic ideal gases and significantly smaller for some gas mixtures. A second dimensionless number,

$$L = k/\rho c_p D = (\delta_\kappa/\delta_D)^2, \tag{5}$$

is a measure of the ratio of thermal to mass-diffusion effects, and is also of order one. Simple ideal-gas kinetic theory predicts σ and L independent of pressure and temperature, which is close to experimental observation.[14]

Since δ_ν, δ_κ, and δ_D are all of comparable size in gases, we can expect that viscous effects and mass-diffusion effects may be important whenever thermoacoustic effects are important.

II. THE OSCILLATING VARIABLES

We consider sound propagating in the x direction in a uniformly mixed two-component ideal gas within a channel with constant cross sectional area A and hydraulic[15] radius r_h much larger than the viscous, thermal, and diffusion penetration depths but much smaller than the acoustic wavelength. We adopt the common[8] complex notation for time-oscillating quantities (pressure p, temperature T, vector velocity $\mathbf{v}$ with component u parallel to x and component v perpendicular to x, density ρ, mass fraction c, entropy per unit mass s):

$$p = p_m + \text{Re}[p_1(x)e^{i\omega t}] + \cdots, \tag{6}$$

$$u = \text{Re}[u_1(x,y)e^{i\omega t}] + \cdots, \tag{7}$$

$$T = T_m + \text{Re}[T_1(x,y)e^{i\omega t}] + \cdots, \tag{8}$$

$$\rho, c, s, \text{ etc.} = \text{similar to } T, \tag{9}$$

$$\mathbf{v}, v = \text{similar to } u. \tag{10}$$

In this monofrequency, steady-state acoustic approximation, all the time dependence appears in the factor $e^{i\omega t}$. The mean values (subscript m) are real, but the small amplitudes (subscript 1) are in general complex to account for the time phasing of the oscillating quantities. The coordinate y measures the distance from the wall.

To establish notation and method, we begin by deriving the well-known y dependence of the gas velocity,[16] using the x-component of the momentum equation, for which our acoustic approximation is

$$i\omega\rho_m u_1 = -\frac{dp_1}{dx} + \frac{\mu}{}\frac{\partial^2 u_1}{\partial y^2}. \tag{11}$$

The momentum equation for a gas mixture is identical to that of a pure gas. The x derivatives of u_1 have been neglected because they are of order u_1/λ, and hence are much smaller than the y derivatives, of order u_1/δ_ν. Equation (11) is an ordinary differential equation for $u_1(y)$. With boundary condition $u_1(0)=0$ at the solid surface, its boundary-layer solution is

$$u_1 = \frac{i}{\omega\rho_m}[1 - e^{-(1+i)y/\delta_\nu}]\frac{dp_1}{dx}. \tag{12}$$

Later, we will need the spatial average of Eq. (12) over the cross section A of the channel:

$$\langle u_1 \rangle = \frac{i}{\omega\rho_m}(1-f_\nu)\frac{dp_1}{dx}, \tag{13}$$

where $\langle\,\rangle$ denotes the spatial average over A and

$$f_\nu = (1-i)\delta_\nu/2r_h \tag{14}$$

is the spatial average of the exponential. Combining Eqs. (12) and (13) gives another useful expression for the velocity,

$$u_1 = \frac{\langle u_1 \rangle}{1-f_\nu}[1 - e^{-(1+i)y/\delta_\nu}]. \tag{15}$$

To find the dependence of the oscillating temperature T on y is complicated in a gas mixture, because thermal diffusion couples the oscillations of temperature and concentration. Following Landau and Lifshitz,[17] let the concentration c be the local mass fraction of the lighter component; i.e., c is the ratio of the mass of the component with the lower molecular weight to the total mass of gas, per unit volume. Then the convective mass flux density of this component is $\rho c\mathbf{v}$, and the diffusive mass flux density of this component is

$$\mathbf{i} = -\rho D[\nabla c + (k_T'/T)\nabla T], \tag{16}$$

with barodiffusion neglected. The diffusion coefficient D gives diffusion in response to a concentration gradient, and the thermal diffusion ratio k_T' gives the diffusion in response to a temperature gradient. Using Eq. (16) with Eq. (57.3) of Landau and Lifshitz,

$$\rho(\partial c/\partial t + \mathbf{v}\cdot\nabla c) = -\nabla\cdot\mathbf{i}, \tag{17}$$

to eliminate $\mathbf{i}$ yields

$$(\partial c/\partial t + \mathbf{v}\cdot\nabla c) = \nabla\cdot[D\nabla c + (Dk_T'/T)\nabla T]. \tag{18}$$

This equation shows that the concentration at a point changes in time due to convection of a concentration gradient past that point plus diffusion caused by both a concentration gradient and a temperature gradient. Using Eqs. (6)–(10) for all variables, keeping terms to first order, and realizing that $dc_m/dx=0$ for a well-mixed gas, Eq. (18) becomes simply

$$c_1 = \frac{\delta_D^2}{2i}\left[\frac{\partial^2 c_1}{\partial y^2} + \frac{k_T'}{T_m}\frac{\partial^2 T_1}{\partial y^2}\right]. \tag{19}$$

To examine oscillating heat transfer in the mixture, we begin by combining Eqs. (57.6) and (58.12) of Landau and Lifshitz, eliminating $\mathbf{q} - g\mathbf{i}$, substituting Eqs. (6)–(10), and keeping terms to first order:

$$\rho_m T_m\left(i\omega s_1 + u_1\frac{ds_m}{dx}\right)$$
$$= k\frac{\partial^2 T_1}{\partial y^2} - \left[k_T'\left(\frac{\partial g}{\partial c}\right)_{p,T} - T_m\left(\frac{\partial g}{\partial T}\right)_{p,c}\right]\nabla\cdot\mathbf{i}_1, \tag{20}$$

where $\mathbf{q}$ is the heat flux density and g is the chemical potential per unit mass. Equation (17) shows that $\nabla\cdot\mathbf{i}_1 = -i\omega\rho_m c_1$. We have $ds_m/dx=0$ in the present simple problem, although this will not be the case when $dT_m/dx \neq 0$ in the stacks of thermoacoustic engines and refrigerators, nor when $dc_m/dx\neq 0$ in apparatus with substantial net mixture separation. We eliminate s_1 using

$$ds = \left(\frac{\partial s}{\partial T}\right)_{p,c}dT + \left(\frac{\partial s}{\partial c}\right)_{p,T}dc + \left(\frac{\partial s}{\partial p}\right)_{T,c}dp \tag{21}$$

$$= \frac{c_p}{T}dT - \left(\frac{\partial g}{\partial T}\right)_{p,c}dc - \frac{1}{\rho T}dp, \tag{22}$$

where we have used two Maxwell relations and the ideal-gas equation of state. With these substitutions, Eq. (20) becomes

$$T_1 = \frac{p_1}{\rho_m c_p} + \frac{\varepsilon T_m c_1}{k_T'} + \frac{\delta_\kappa^2}{2i} \frac{\partial^2 T_1}{\partial y^2}, \tag{23}$$

using the definition

$$\varepsilon = \frac{(k_T')^2}{T_m c_p} \left(\frac{\partial g}{\partial c} \right)_{p,T} \tag{24}$$

for future simplicity.

Equations (19) and (23) comprise two coupled differential equations in the unknown functions $c_1(y)$ and $T_1(y)$. In general, the solid has sufficient heat capacity and thermal conductivity to enforce

$$T_1(0) = 0 \tag{25}$$

on the gas at the solid surface, so this provides one boundary condition for the solution. The other boundary condition is obtained from the fact that, absent condensation and evaporation at the solid, the first-order concentration flux density perpendicular to the wall must be zero, which yields

$$\left. \frac{\partial c_1}{\partial y} \right|_0 + \frac{k_T'}{T_m} \left. \frac{\partial T_1}{\partial y} \right|_0 = 0. \tag{26}$$

Equations (19) and (23) are very similar to Eqs. (58.14) and (58.15) of Landau and Lifshitz, and are simplified versions of Eqs. (5) and (3) of Raspet et al.[6] if we also use our results for ε and k_T' (see next section). However, the present problem differs significantly from that of Raspet et al. in two ways. First, our boundary condition Eq. (26) allows no flux of either component into the wall, while their "wet" boundary condition allows flux of their condensing component into the wall by ensuring that the partial pressure of the condensing component is constant at the wall. Second, we keep the k_T' term in Eq. (19) while they neglect it in their Eq. (28).

To solve Eqs. (19) and (23), subject to the boundary conditions given by Eqs. (25) and (26), we can use Eq. (23) to eliminate c_1 from the other equations, obtaining a fourth-order differential equation for T_1 with two boundary conditions:

$$T_1 = \frac{p_1}{\rho_m c_p} + \frac{1}{2i} [\delta_\kappa^2 + (1+\varepsilon)\delta_D^2] \frac{\partial^2 T_1}{\partial y^2} + \frac{\delta_\kappa^2 \delta_D^2}{4} \frac{\partial^4 T_1}{\partial y^4}, \tag{27}$$

$$T_1(0) = 0, \tag{28}$$

$$(1+\varepsilon) \left. \frac{\partial T_1}{\partial y} \right|_0 - \frac{\delta_\kappa^2}{2i} \left. \frac{\partial^3 T_1}{\partial y^3} \right|_0 = 0. \tag{29}$$

An additional boundary condition is simply that T_1 must remain finite as $y \to \infty$. The solution is

$$T_1 = \frac{p_1}{\rho_m c_p} [1 - C e^{-(1+i)y/\delta_{\kappa D}} - (1-C) e^{-(1+i)y/\delta_{D\kappa}}], \tag{30}$$

where

$$\delta_{\kappa D}^2 = \tfrac{1}{2} \delta_\kappa^2 [1 + (1+\varepsilon)/L + \sqrt{[1+(1+\varepsilon)/L]^2 - 4/L}\,], \tag{31}$$

$$\delta_{D\kappa}^2 = \tfrac{1}{2} \delta_\kappa^2 [1 + (1+\varepsilon)/L - \sqrt{[1+(1+\varepsilon)/L]^2 - 4/L}\,], \tag{32}$$

$$C = \frac{\sqrt{L}\,\delta_{\kappa D} - \delta_{D\kappa}}{(1+\sqrt{L})(\delta_{\kappa D} - \delta_{D\kappa})}, \tag{33}$$

which can be verified with modest difficulty by direct substitution into Eqs. (27)–(29). [The identities

$$\frac{\delta_{\kappa D}^2}{\delta_\kappa^2} + \frac{\delta_{D\kappa}^2}{\delta_\kappa^2} = 1 + \frac{1+\varepsilon}{L}, \tag{34}$$

$$L \delta_{\kappa D}^2 \delta_{D\kappa}^2 = \delta_\kappa^4, \tag{35}$$

obtained by manipulating Eqs. (31) and (32), and the algebra identity

$$\delta_{\kappa D}^3 \pm \delta_{D\kappa}^3 = (\delta_{\kappa D} \pm \delta_{D\kappa})(\delta_{\kappa D}^2 + \delta_{D\kappa}^2 \mp \delta_{\kappa D}\delta_{D\kappa}), \tag{36}$$

are useful when working through some of the tedious steps in the derivations in this paper.] Note that $\varepsilon \to 0$ recovers the usual thermoacoustic solution: When $L \gg 1$, $\delta_{\kappa D} \to \delta_\kappa$, $\delta_{D\kappa} \to \delta_D$, and $C \to 1$; or when $L < 1$, $\delta_{\kappa D} \to \delta_D$, $\delta_{D\kappa} \to \delta_\kappa$, and $C \to 0$. The spatial average of the temperature over the cross-sectional area of the channel is

$$\langle T_1 \rangle = \frac{p_1}{\rho_m c_p} [1 - C f_{\kappa D} - (1-C) f_{D\kappa}], \tag{37}$$

where

$$f_{\kappa D} = (1-i)\delta_{\kappa D}/2r_h \tag{38}$$

and similarly for $f_{D\kappa}$.

III. TYPICAL VALUES

To present some typical numerical values, we consider He–Ar and He–Xe mixtures, which are of interest in thermoacoustic refrigerators.[11,12] Although the derivation elsewhere in this paper follows Landau and Lifshitz's notational preference for mass fraction c, most data are tabulated in terms of mole fraction n; the two are related by

$$c = \frac{n_L m_L}{n_L m_L + (1-n_L)m_H}, \tag{39}$$

where m is molar mass and the subscripts refer to the lighter and heavier species. We use viscosity and thermal conductivity calculations from Giacobbe[18] at 20 °C, and mass diffusion coefficients interpolated to 20 °C from the measurements of Srivastava[19], which are in good agreement with calculations. We also include the weak concentration dependence of D according to the recommendations of Chapman and Cowling.[20] Based on these data, σ and L are shown in Fig. 2(a).

Next we need ε, which requires evaluation of $(\partial g/\partial c)_{p,T}$. Landau and Lifshitz suggest how to proceed. The chemical potential g (per unit mass) is

$$g = \hat{g}_L/m_L - \hat{g}_H/m_H, \tag{40}$$

where the caret indicates a molar chemical potential. For ideal gases, we have

$$\hat{g}_L = \hat{g}_{L,\text{pure}} + RT \ln n_L, \tag{41}$$

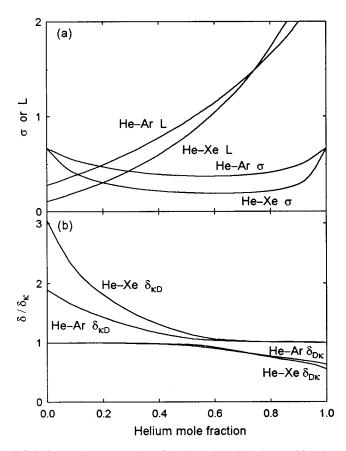$$\hat{g}_H = \hat{g}_{H,\text{pure}} + RT \ln(1 - n_L), \tag{42}$$

FIG. 2. Some relevant properties of He–Ar and He–Xe mixtures. (a) Values of σ and L, giving the ratios $\delta_\nu^2/\delta_\kappa^2$ and $\delta_\kappa^2/\delta_D^2$, respectively. (b) The ratios $\delta_{\kappa D}/\delta_\kappa$ and $\delta_{D\kappa}/\delta_\kappa$, which appear throughout our calculations. Each of these approaches 1 and $1/\sqrt{L}$ in the two pure-gas limits.

with R the universal gas constant. Using Eqs. (39)–(42), it is straightforward to compute

$$\left(\frac{\partial g}{\partial c}\right)_{p,T} = \left(\frac{\partial g}{\partial n_L}\right)_{p,T} \bigg/ \left(\frac{\partial c}{\partial n_L}\right)_{p,T}$$
$$= \frac{RT}{c(1-c)[m_L + c(m_H - m_L)]}. \tag{43}$$

We must also convert from Landau and Lifshitz's thermal diffusion ratio k_T' to the thermal diffusion ratio k_T used in most other treatments. These differ by a factor of dc/dn_L, so that

$$k_T' = k_T \frac{m_L m_H}{[n_L m_L + (1 - n_L) m_H]^2}$$
$$= k_T \frac{[m_L + (m_H - m_L)c]^2}{m_L m_H}. \tag{44}$$

Combining Eqs. (24), (43), and (44) we have finally

$$\varepsilon = \frac{\gamma - 1}{\gamma} \frac{k_T^2}{n_L(1 - n_L)}, \tag{45}$$

where γ is the ratio of isobaric to isochoric specific heats.

For k_T, we use the experimental data of Atkins et al.,[21] ranging over helium mole fractions $0.1 \leq n_L \leq 0.5$. To interpolate and extrapolate elsewhere, we fit their data with $k_T = 0.38 n_L^{1.2} (1 - n_L)^{0.8}$ for He–Ar and $k_T = 0.40 n_L^{1.3} (1 - n_L)^{0.7}$ for He–Xe, which give better fits to the data than
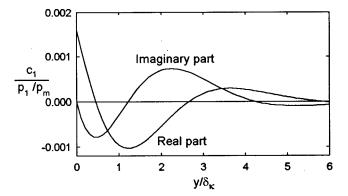

FIG. 3. Real and imaginary parts of c_1, normalized by p_1/p_m, for a He–Xe mixture with $n_L = 0.50$. For this mixture, $\delta_\mu/\delta_\kappa = 0.445$, $\delta_{\kappa D}/\delta_\kappa = 1.16$, and $\delta_{D\kappa}/\delta_\kappa = 0.97$.

the functional form $n_L(1 - n_L)$ suggested by the simplest kinetic theory. Figure 2(b) shows the resulting values of $\delta_{\kappa D}$ and $\delta_{D\kappa}$. Clearly Fig. 1 was unrealistically naive. Heat and mass diffusion are so intimately linked that the length scales $\delta_{\kappa D}$ and $\delta_{D\kappa}$ appearing in $T_1(y)$ are very different from the familiar δ_κ. Hence, it is also clear that correct calculations of enthalpy flux, proportional to $\text{Re}[T_1 \tilde{u}_1]$, must include thermal diffusion. (The tilde denotes complex conjugation.)

We can use Eqs. (23) and (30) to obtain $c_1(y)$, which is plotted in Fig. 3 for a 50–50 He–Xe mixture. The imaginary part is negative for $y \lesssim \delta_\kappa$ and is positive for $\delta_\kappa \lesssim y \lesssim 4\delta_\kappa$, which is qualitatively consistent with the phenomena we described in Fig. 1, where the thermal diffusion occurs during pressure extrema of Fig. 1(a) and (c) so that the mixture is most separated in Fig. 1(b) and (d). However, the large $\text{Re}[c_1]$ in Fig. 3 shows again that this oscillating thermal diffusion is much richer than we had anticipated in Fig. 1.

IV. BOUNDARY-LAYER MASS SEPARATION

The phased oscillating phenomena described above cause a time-averaged mass separation, whose origin is easy to understand qualitatively. The oscillating temperature gradient $\partial T_1/\partial y$ near the wall causes nonzero concentration oscillations near the wall. At this distance from the wall, comparable to δ_ν, the oscillating velocity u_1 in the x direction depends on y. If the time phasing is favorable, this produces a time-averaged mass flux density $\overline{\rho c u}$ of the lighter component and $\overline{\rho(1-c)u}$ of the heavier component in the x direction, while the total mass flux density $\overline{\rho u}$ remains zero. (The overbar signifies time average.) Exaggerating the magnitudes of the effects, we could imagine that during one half of the cycle the light component would be stuck deep in the viscous boundary layer and the heavy component would be free to move outside the viscous boundary layer; during the other half of the cycle the roles would be reversed, with the heavy component immobilized by viscosity and the lighter component free to move. If the velocity were phased correctly with respect to this oscillating concentration, the time-averaged result would be flux of the light component in one direction along x and flux of the heavy component in the opposite direction.

The time-averaged second-order mass flux of the lighter component is

$$A\langle \overline{\rho c u}\rangle_2 = \frac{A\rho_m}{2}\text{Re}[\langle c_1 \tilde{u}_1 \rangle]. \qquad (46)$$

To evaluate the right-hand side, we use Eq. (23) for $c_1(y)$, Eq. (30) for $T_1(y)$, and Eq. (15) for $u_1(y)$. The spatial average $\langle c_1 \tilde{u}_1 \rangle$ involves boundary-layer-approximation integrals of the form

$$\frac{1}{r_h}\int_0^{r_h} e^{-(1+i)y/\delta}[1 - e^{-(1-i)y/\delta_\nu}]\, dy = \frac{(\delta - \delta_\nu) - i(\delta + \delta_\nu)}{2r_h(1 + \delta_\nu^2/\delta^2)}, \qquad (47)$$

where δ is either $\delta_{\kappa D}$ or $\delta_{D\kappa}$. After tedious algebra leading to an intermediate result,

$$\langle \overline{\rho c u}\rangle_2 = \frac{\delta_\kappa}{4r_h}\frac{k_T'/\varepsilon}{c_p T_m}\text{Re}\left[\frac{p_1\langle \tilde{u}_1\rangle}{(1-\tilde{f}_\nu)}\left\{ C\left(1 - \frac{\delta_{\kappa D}^2}{\delta_\kappa^2}\right)\right.\right.$$

$$\times \frac{(\delta_{\kappa D}/\delta_\kappa - \sqrt{\sigma}) - i(\delta_{\kappa D}/\delta_\kappa + \sqrt{\sigma})}{\delta_{\kappa D}^2/\delta_\kappa^2 + \sigma} + (1 - C)$$

$$\left.\left.\times\left(1 - \frac{\delta_{D\kappa}^2}{\delta_\kappa^2}\right)\frac{(\delta_{D\kappa}/\delta_\kappa - \sqrt{\sigma}) - i(\delta_{D\kappa}/\delta_\kappa + \sqrt{\sigma})}{\delta_{D\kappa}^2/\delta_\kappa^2 + \sigma}\right\}\right], \qquad (48)$$

the final result is

$$A\langle \overline{\rho c u}\rangle_2 = \frac{\delta_\kappa}{4r_h}\frac{k_T'}{c_p T_m}(F_{\text{trav}}\text{Re}[p_1\tilde{U}_1] + F_{\text{stand}}\text{Im}[p_1\tilde{U}_1]) \qquad (49)$$

to lowest order in δ/r_h, where $U_1 = A\langle u_1\rangle$ is the volume flow rate. The traveling-wave and standing-wave factors are given by

$$F_{\text{trav}} = \frac{\sigma\sqrt{\sigma L} - \sqrt{\sigma} - \sigma\sqrt{L}(\delta_{\kappa D}/\delta_\kappa + \delta_{D\kappa}/\delta_\kappa)}{(1+\sqrt{L})[1+\sigma(1+L+\varepsilon+\sigma L)]}, \qquad (50)$$

$$F_{\text{stand}} = \frac{-\sigma\sqrt{\sigma L} + \sqrt{\sigma} - \sigma\sqrt{L}(\delta_{\kappa D}/\delta_\kappa + \delta_{D\kappa}/\delta_\kappa)}{(1+\sqrt{L})[1+\sigma(1+L+\varepsilon+\sigma L)]}. \qquad (51)$$

Equation (49) can be rewritten in terms of molar quantities:

$$\dot{N}_{L,2} = \frac{\delta_\kappa}{4r_h}\frac{\gamma-1}{\gamma}\frac{k_T}{RT_m}(F_{\text{trav}}\text{Re}[p_1\tilde{U}_1] + F_{\text{stand}}\text{Im}[p_1\tilde{U}_1]), \qquad (52)$$

where $\dot{N}_{L,2}$ is the rate at which moles of the light component move in the x direction. [Note k_T' in Eq. (49); k_T in Eq. (52).]

Figure 4 shows $k_T F$ for He–Ar and He–Xe mixtures. The factors in Eq. (52) can be grouped into dimensionless ratios, showing that the average molar separation flux density in the channel scales like the product of p_1/p_m, $\langle u_1\rangle/a$, a, δ_κ/r_h, $(\gamma-1)/4\gamma$, and the molar density N/V. The details, captured in $k_T F_{\text{trav}}$ and $k_T F_{\text{stand}}$, reduce the magnitude of the effect by roughly 10^{-2}, as shown in Fig. 4. Hence, with $(\gamma-1)/4\gamma \sim 10^{-1}$, the molar separation flux in a short porous medium having $r_h \sim \delta_\kappa$ could be of order $10^{-3}M^2(N/V)aA$

(where $M \sim |p_1|/p_m \sim |\langle u_1\rangle|/a$ is the acoustic Mach number). If such a short porous medium filled the cross section of a chamber whose length was of the order of the acoustic wavelength, and if nonzero dc_m/dx did little to change this mass separation rate, then a substantial concentration difference could establish itself in a time of order $1/10^{-3}M^2 f$, where f is the frequency of the wave. Hence, it seems likely that thermoacoustic refrigerators using gas mixtures might have concentration differences across their stacks, if bulk gas motion such as convection or streaming does not re-mix the gases with sufficient vigor.

Figure 4 also shows that traveling-wave phasing should be more effective than standing-wave phasing at separating the mixture, reconfirming that our initial view of this process, illustrated in Fig. 1, was much too naive.

V. BOUNDARY-LAYER ACOUSTIC POWER DISSIPATION

To find the time-averaged acoustic power $d\dot{E}_2$ dissipated in a length dx of the channel, we write

$$\frac{d\dot{E}}{dx} = -A\frac{d\langle \overline{pu}\rangle}{dx}. \qquad (53)$$

Expressing Eq. (53) in complex notation and expanding the derivative gives

$$\frac{d\dot{E}_2}{dx} = -\frac{1}{2}A\,\text{Re}\left[\langle \tilde{u}_1\rangle\frac{dp_1}{dx} + \tilde{p}_1\frac{d\langle u_1\rangle}{dx}\right]. \qquad (54)$$

We can obtain dp_1/dx from Eq. (13) above. To find $d\langle u_1\rangle/dx$, we use the continuity equation $\partial\rho/\partial t + \nabla\cdot(\rho\mathbf{v}) = 0$, which can be averaged with respect to y in our acoustic approximation to obtain

$$i\omega\langle\rho_1\rangle + \rho_m d\langle u_1\rangle/dx = 0. \qquad (55)$$

Using $d\rho = -(\rho/T)\,dT + (\gamma/a^2)\,dp$, we can express the spatially averaged density as $\langle\rho_1\rangle = -(\rho_m/T_m)\langle T_1\rangle + (\gamma/a^2)p_1$. Substituting this into Eq. (55), using Eq. (37) for $\langle T_1\rangle$, and eliminating c_p by means of the thermodynamic identity $\gamma - 1 = a^2/Tc_p$ yields
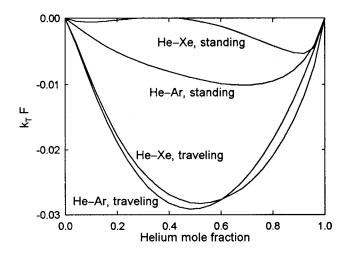

FIG. 4. Dimensionless molar-separation-flux parameters $k_T F_{\text{trav}}$ and $k_T F_{\text{stand}}$ for He–Ar and He–Xe mixtures.
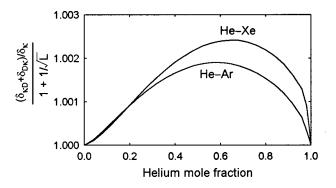
FIG. 5. The factor by which thermal diffusion multiplies boundary-layer thermal-relaxation dissipation of acoustic power, for He–Ar and He–Xe mixtures.

$$i\omega\{1+(\gamma-1)[Cf_{\kappa D}+(1-C)f_{D\kappa}]\}p_1$$

$$+\rho_m a^2\,d\langle u_1\rangle/dx=0 \tag{56}$$

as an acoustic expression of the continuity equation which can be solved for $d\langle u_1\rangle/dx$.

Finally, substituting Eqs. (56) and (13) into Eq. (54), we obtain

$$\frac{d\dot{E}_2}{dx}=\frac{A\omega}{2}\left[\frac{\rho_m|\langle u_1\rangle|^2}{|1-f_\nu|^2}\mathrm{Im}[-f_\nu]\right.$$

$$\left.+\frac{(\gamma-1)|p_1|^2}{\rho_m a^2}\mathrm{Im}[-Cf_{\kappa D}-(1-C)f_{D\kappa}]\right]. \tag{57}$$

The first term gives the viscous damping of sound and the second term gives the complicated thermal damping in the presence of thermal diffusion. Using the definition[15] of hydraulic radius, Eq. (57) reduces to

$$\frac{d\dot{E}_2}{dS}=\frac{1}{4}\rho_m|\langle u_1\rangle|^2\omega\delta_\nu$$

$$+\frac{1}{4}\frac{|p_1|^2}{\rho_m a^2}(\gamma-1)\omega\frac{(\delta_{\kappa D}+\delta_{D\kappa})}{1+1/\sqrt{L}}, \tag{58}$$

to lowest order in the δ's, where S is the surface area of the channel. The first term is the familiar[8] boundary-layer viscous dissipation per unit surface area; it is unchanged by thermal diffusion. The second term represents the combined dissipative effects of heat and mass diffusion. The limit $\varepsilon \to 0$ recovers the usual[8] thermoacoustic solution, with the final fraction in the second term of Eq. (58) reducing simply to δ_κ. (The similar-looking result in Ref. 2 does not recover the usual thermoacoustic solution when $k_T\to 0$.)

Figure 5 displays this final fraction in the second term of Eq. (58) for He–Ar and He–Xe mixtures, divided by δ_κ, so this figure shows the ratio of the present p^2 dissipation term to the pure-gas p^2 term involving only δ_κ. The extra dissipation is less than one percent for these mixtures, so it is unlikely that this effect would have been noticed in measurements to date with thermoacoustic refrigerators. However, such refrigerators operate with a nonzero dT_m/dx, and presumably also with a nonzero dc_m/dx; these effects might increase the mass-diffusion dissipation.

[1] P. S. Spoor and G. W. Swift, ''Mode locking of acoustic resonators and its application to vibration cancellation in acoustic heat engines,'' J. Acoust. Soc. Am. **106**, 1353–1362 (1999).

[2] A. M. Dykhne, A. F. Pal', V. D. Pis'mennyi, V. V. Starostin, and M. D. Taran, ''Dynamics of gas-mixtures separation in the field of a sound wave,'' Zh. Eksp. Teor. Fiz. **88**, 1976–1983 (1985). [English translation: Sov. Phys. JETP **61**, 1171–1175 (1985).]

[3] V. B. Bozhdankevich, A. M. Dykhne, A. F. Pal', V. D. Pis'mennyi, V. V. Pichugin, A. N. Starostin, and M. D. Taran, ''Thermodiffusional separation of gas mixtures in the field of a sound wave,'' Dokl. Akad. Nauk SSSR **288**, 605–608 (1986). [English translation: Sov. Phys. Dokl. **31**, 428–430 (1986).]

[4] W. L. M. Nyborg, ''Acoustic streaming,'' in *Physical Acoustics, Volume IIB*, edited by W. P. Mason (Academic, New York, 1965), pp. 265–331.

[5] G. W. Howell, ''Separation of isotopes by oscillatory flow,'' Phys. Fluids **31**, 1803–1805 (1988).

[6] R. Raspet, C. J. Hickey, and J. M. Sabatier, ''The effect of mass transfer on sound propagation in cylindrical tubes using the low reduced frequency approximation,'' J. Acoust. Soc. Am. **105**, 65–73 (1999).

[7] D. M. Ruthven, Ed., *Encyclopedia of Separation Technology* (Wiley, New York, 1997).

[8] G. W. Swift, ''Thermoacoustic engines,'' J. Acoust. Soc. Am. **84**, 1145–1180 (1988).

[9] R. S. Reid, W. C. Ward, and G. W. Swift, ''Cyclic thermodynamics with open flow,'' Phys. Rev. Lett. **80**, 4617–4620 (1998).

[10] K. F. Herzfeld and T. A. Litovitz, *Absorption and Dispersion of Ultrasonic Waves* (Academic, New York, 1959).

[11] S. L. Garrett, J. A. Adeff, and T. J. Hofler, ''Thermoacoustic refrigerator for space applications,'' AAIA J. Thermophys. Heat Trans. **7**, 595–599 (1993).

[12] M. E. Poese, ''Performance measurements on a thermoacoustic refrigerator driven at high amplitudes, Master's thesis, The Pennsylvania State University, 1998. Applied Research Laboratory.

[13] W. C. Ward and G. W. Swift, ''Design environment for low amplitude thermoacoustic engines (DeltaE),'' J. Acoust. Soc. Am. **95**, 3671–3672 (1994). Fully tested software and user's guide available from Energy Science and Technology Software Center, U.S. Department of Energy, Oak Ridge, Tennessee. To review DeltaE's capabilities, visit the Los Alamos thermoacoustics web site at www.lanl.gov/thermoacoustics/. For a beta-test version, contact ww@lanl.gov (Bill Ward) or swift@lanl.gov (Greg Swift) by email.

[14] J. O. Hirschfelder, C. F. Curtiss, and R. B. Bird, *Molecular Theory of Gases and Liquids* (Wiley, New York, 1954).

[15] The hydraulic radius is the ratio of gas volume to gas-solid contact surface area.

[16] N. Rott, ''Damped and thermally driven acoustic oscillations in wide and narrow tubes,'' Z. Angew. Math. Phys. **20**, 230–243 (1969).

[17] L. D. Landau and E. M. Lifshitz, *Fluid Mechanics* (Pergamon, New York, 1982).

[18] F. W. Giacobbe, ''Estimation of Prandtl numbers in binary mixtures of helium and other noble gases,'' J. Acoust. Soc. Am. **96**, 3568–3580 (1994).

[19] K. P. Srivastava, ''Mutual diffusion of binary mixtures of helium, argon, and xenon at different temperatures,'' Physica (Utrecht) **25**, 571–578 (1959).

[20] S. Chapman and T. G. Cowling, *The Mathematical Theory of Non-Uniform Gases* (Cambridge University Press, Cambridge, 1939).

[21] B. E. Atkins, R. E. Bastick, and T. L. Ibbs, ''Thermal diffusion in mixtures of inert gases,'' Proc. R. Soc. London, Ser. A **172**, 142–158 (1939).

1800   J. Acoust. Soc. Am., Vol. 106, No. 4, Pt. 1, October 1999

G. W. Swift and P. S. Spoor: Diffusion and mixture separation   1800

Erratum: "Thermal diffusion and mixture separation in the acoustic boundary layer" [J. Acoust. Soc. Am. 106, 1794–1800 (1999)]

G. W. Swift and P. S. Spoor

Condensed Matter and Thermal Physics Group, Los Alamos National Laboratory, Los Alamos, New Mexico 87545

Our arbitrary decision to let c represent the mass fraction of the *lighter* component was very unfortunate, because it caused k_T' to be *negative* for typical gas mixtures such as He–Ar, in contradiction to the sign convention for k_T used in most publications and in our own numerical examples. Hence, for consistency within this paper and with most publications: In the third paragraph of Sec. II and the first two paragraphs of Sec. IV, the words "lighter" and "heavier" should be interchanged, and "lower" should be "higher." Subscripts H and L should be interchanged in and near Eqs. (39), (40), (43), (44), and (52). [Equations (41), (42), and (45) are unchanged because $n_H = 1 - n_L$.]

Erratum: "Thermal diffusion and mixture separation in the acoustic boundary layer" [J. Acoust. Soc. Am. 106, 1794–1800 (1999)]

G. W. Swift and P. S. Spoor

Condensed Matter and Thermal Physics Group, Los Alamos National Laboratory, Los Alamos, New Mexico 87545

In the first paragraph of Sec. IV, the statement ''...while the total mass flux density $\overline{\rho u}$ remains zero'' is wrong. In the situation we are considering, with sealed reservoirs at the ends of the channel, the total time-averaged *mole* flux is zero, as the mole flux of the heavy component in one direction equals that of the light component in the other direction. Hence, nonzero net mass must flow in the direction that the heavy component flows.

It is easy to show that this net time-averaged second-order mass flux is

$$\dot{M}_2 = \dot{M}_{H,2}(1 - m_L/m_H) \tag{46a}$$

when the mole fluxes are equal and opposite, and that the time-averaged second-order mass flux of the heavy component is

$$\dot{M}_{H,2} \equiv A\overline{\langle \rho c u \rangle_2} = \frac{A\rho_m}{2}\,\mathrm{Re}[\langle c_1 \widetilde{u_1} \rangle] + c_m \dot{M}_2. \tag{46b}$$

These equations should replace Eq. (46) in the manuscript. Equations (48) and (49) give expressions for $\rho_m\,\mathrm{Re}[\langle c_1 \widetilde{u_1} \rangle]/2$, not for $\langle \rho c u \rangle_2$.

Finally, by combining Eqs. (46a) and (46b) to eliminate $\dot{M}_2$ and solving for $\dot{M}_{H,2} \equiv m_H \dot{N}_{H,2}$, we arrive at Eq. (52), which is correct as written.

We are grateful to Drew Geller for bringing this error to our attention.